

## Data-based perfect-deficit approach to understanding climate extremes and forest carbon assimilation capacity

This content has been downloaded from IOPscience. Please scroll down to see the full text.

2014 Environ. Res. Lett. 9 065002

(<http://iopscience.iop.org/1748-9326/9/6/065002>)

View [the table of contents for this issue](#), or go to the [journal homepage](#) for more

Download details:

IP Address: 134.74.14.82

This content was downloaded on 03/06/2014 at 12:11

Please note that [terms and conditions apply](#).

# Data-based perfect-deficit approach to understanding climate extremes and forest carbon assimilation capacity

Suhua Wei<sup>1,2</sup>, Chuixiang Yi<sup>1,2</sup>, George Hendrey<sup>1,2</sup>, Timothy Eaton<sup>1,2</sup>, Gerald Rustic<sup>1,2</sup>, Shaoqiang Wang<sup>3</sup>, Heping Liu<sup>4</sup>, Nir Y Krakauer<sup>5,2</sup>, Weiguo Wang<sup>6</sup>, Ankur R Desai<sup>7</sup>, Leonardo Montagnani<sup>8</sup>, Kyaw Tha Paw U<sup>9</sup>, Matthias Falk<sup>9</sup>, Andrew Black<sup>10</sup>, Christian Bernhofer<sup>11</sup>, Thomas Grünwald<sup>11</sup>, Tuomas Laurila<sup>12</sup>, Alessandro Cescatti<sup>13</sup>, Eddy Moors<sup>14</sup>, Rosvel Bracho<sup>15</sup> and Riccardo Valentini<sup>16</sup>

<sup>1</sup> School of Earth and Environmental Sciences, Queens College, City University of New York, New York, NY 11367, USA

<sup>2</sup> Graduate Center, City University of New York, New York, NY 10016, USA

<sup>3</sup> Institute of Geographic Sciences and Natural Resource Research, Chinese Academy of Science, Beijing 100101, People's Republic of China

<sup>4</sup> Laboratory for Atmospheric Research, Department of Civil and Environmental Engineering, Washington State University, Pullman, WA 99164, USA

<sup>5</sup> Civil Engineering Department and NOAA-CREST, City College, City University of New York, New York, NY 10031, USA

<sup>6</sup> Environmental Modeling Center, National Centers for Environmental Prediction, NOAA, 5835 University Research Court, College Park, MD 20740, USA

<sup>7</sup> Center for Climatic Research, Nelson Institute for Environmental Studies, University of Wisconsin-Madison, Madison, WI 53706, USA

<sup>8</sup> Faculty of Science and Technology, Free University of Bolzano, Piazza Università 5, I-39100 Bolzano, Italy

<sup>9</sup> Atmospheric Science Program, Department of Land, Air, and Water Resources, University of California, Davis, CA 95616-8717, USA

<sup>10</sup> Faculty of Land and Food System, The University of British Columbia, Vancouver, Canada BC V6T 1Z4

<sup>11</sup> Institute of Hydrology and Meteorology, Technische Universität Dresden, Piennner Str. 23, D-01737 Tharandt, Germany

<sup>12</sup> Finnish Meteorological Institute, PO Box 503, Sahaajankatu 20E, Helsinki, Finland

<sup>13</sup> Climate Change Unit, Institute for Environment and Sustainability, European Commission, DG Joint Research Centre, Ispra, Italy

<sup>14</sup> Alterra Green World Research, Wageningen, Netherlands

<sup>15</sup> School of Forest Resources and Conservation, University of Florida, Gainesville, Florida, USA

<sup>16</sup> Department of Forest Science and Environment, University of Tuscia, Viterbo, Italy

E-mail: [cyi@qc.cuny.edu](mailto:cyi@qc.cuny.edu)

Received 9 January 2014, revised 27 April 2014

Accepted for publication 2 May 2014

Published 2 June 2014


## Abstract

Several lines of evidence suggest that the warming climate plays a vital role in driving certain types of extreme weather. The impact of warming and of extreme weather on forest carbon assimilation capacity is poorly known. Filling this knowledge gap is critical towards



Content from this work may be used under the terms of the [Creative Commons Attribution 3.0 licence](https://creativecommons.org/licenses/by/3.0/). Any further distribution of this work must maintain attribution to the author(s) and the title of the work, journal citation and DOI.

understanding the amount of carbon that forests can hold. Here, we used a perfect-deficit approach to identify forest canopy photosynthetic capacity (CPC) deficits and analyze how they correlate to climate extremes, based on observational data measured by the eddy covariance method at 27 forest sites over 146 site-years. We found that droughts severely affect the carbon assimilation capacities of evergreen broadleaf forest (EBF) and deciduous broadleaf forest. The carbon assimilation capacities of Mediterranean forests were highly sensitive to climate extremes, while marine forest climates tended to be insensitive to climate extremes. Our estimates suggest an average global reduction of forest CPC due to unfavorable climate extremes of 6.3 Pg C ( $\sim 5.2\%$  of global gross primary production) per growing season over 2001–2010, with EBFs contributing 52% of the total reduction.

 Online supplementary data available from [stacks.iop.org/ERL/9/065002/mmedia](http://stacks.iop.org/ERL/9/065002/mmedia)

Keywords: climate extremes, drought, carbon assimilation capacity, perfect-deficit approach, forests

## 1. Introduction

Forests store  $\sim 45\%$  of terrestrial carbon ( $\sim 1600$  Pg C), contributing  $\sim 50\%$  of terrestrial net primary production (Bonan 2008) and making them significant carbon sinks that can mitigate global warming (Nemani *et al* 2003, Gielen *et al* 2013), an effect which may be dampened by changing climate (Cox *et al* 2000, Friedlingstein *et al* 2006, Zhao and Running 2010, Yi *et al* 2010, 2013). The 2003 heat wave and drought reduced Europe's gross primary production (GPP) by 30%, which reversed the effect of four years of net carbon sequestration (Ciais *et al* 2005). It is expected that such extreme events will increase in frequency and intensity (Meehl, Tebaldi 2004, Mu *et al* 2011, Trenberth 2012). Studying the impacts of climate extremes on the carbon cycle of forests is important to understand carbon-climate feedback mechanisms because even a small shift in the frequency or severity of climate extremes may result in positive feedback to climate warming (Allen *et al* 2010, Serrano *et al* 2013). However, investigations into the impacts of climate extremes on the carbon cycle are still at the rudimentary level. In this study, we applied the perfect-deficit approach of Yi *et al* (2012) to identify extreme values of canopy photosynthetic capacity (CPC) and climate variables from flux tower data. The daily CPC is calculated as the maximum rate of GPP of the day from FLUXNET tower data at 30 min resolution. CPC forms an upper boundary for the instantaneous canopy photosynthetic rates for a specific site-year. It is hypothesized that ecosystem carbon assimilation capacity is only constrained by climate conditions, and thus a perfect CPC (PCPC) is defined as a measure of the maximum carbon assimilation potential for a site given site-specific 'perfect' climate conditions for a particular day of the year over the years for which data were sampled. Deficits of CPC can be readily identified by subtracting CPC curve from the PCPC curve.

We introduced three indices (duration, intensity and severity) to quantitatively evaluate extreme climate impacts on forests carbon assimilation capacity, indicated by CPC deficits. Principal component analysis (PCA) was applied to identify the driving forces of climate-related carbon assimilation reduction.

We used 27 forest sites from Europe, North America and South America, each with at least four years of continuous carbon and water flux records. The represented ecosystem types include evergreen broadleaf forests (EBF), deciduous broadleaf forests (DBF), evergreen needleleaf forests (ENF) and mixed forests (MF). We also utilize the MODIS GPP and land cover datasets covering 2001–2010 to determine the spatial context of changes in forest carbon assimilation at the global scale. Key objectives of this study were: (1) identify the site-inherent 'perfect' conditions for maximal productivity over the observational records; (2) discover patterns in disruption of forest carbon assimilation associated with climatic extremes; and (3) expand the application of the method (Yi *et al* 2012) geographically to large scale estimation of the reduced carbon assimilation caused by climate extremes.

## 2. Methods

### 2.1. Sites and data

**2.1.1. Flux tower data.** We used data from the FLUXNET 'La-Thuile' database. Data have been processed in a standard methodology described in Papale *et al* 2006. The data are storage corrected and  $u^*$  filtered. We used growing season data (May–October) from 27 forest sites, including four EBF, seven DBF, 13 ENF, and three MF (figure 1). These sites have a minimum of four years of continuous (gap-filled) records of GPP and meteorological variables, including temperature ( $T_a$ ), precipitation ( $P$ ), net radiation ( $R_n$ ), vapor pressure deficit (VPD). GPP was partitioned from net ecosystem exchange (NEE) based on nonlinear regression algorithms (Reichstein *et al* (2005)). Evaporative fraction is calculated from measured latent heat (LE) and sensible heat (H). EF is represented by the ratio between LE and the sum of sensible and LE fluxes:  $EF = LE / (LE + H)$ . This can be also written as  $EF = LE / (R_n - G)$ , where  $R_n$  is net radiation,  $G$  is ground heat flux, and  $R_n - G$  is available energy. If the near soil surface moisture declines, less energy will be used for vaporization, resulting in low EF. In contrast, if adequate water is available for plants due to sufficient precipitation or root access to groundwater, the amount of energy used for

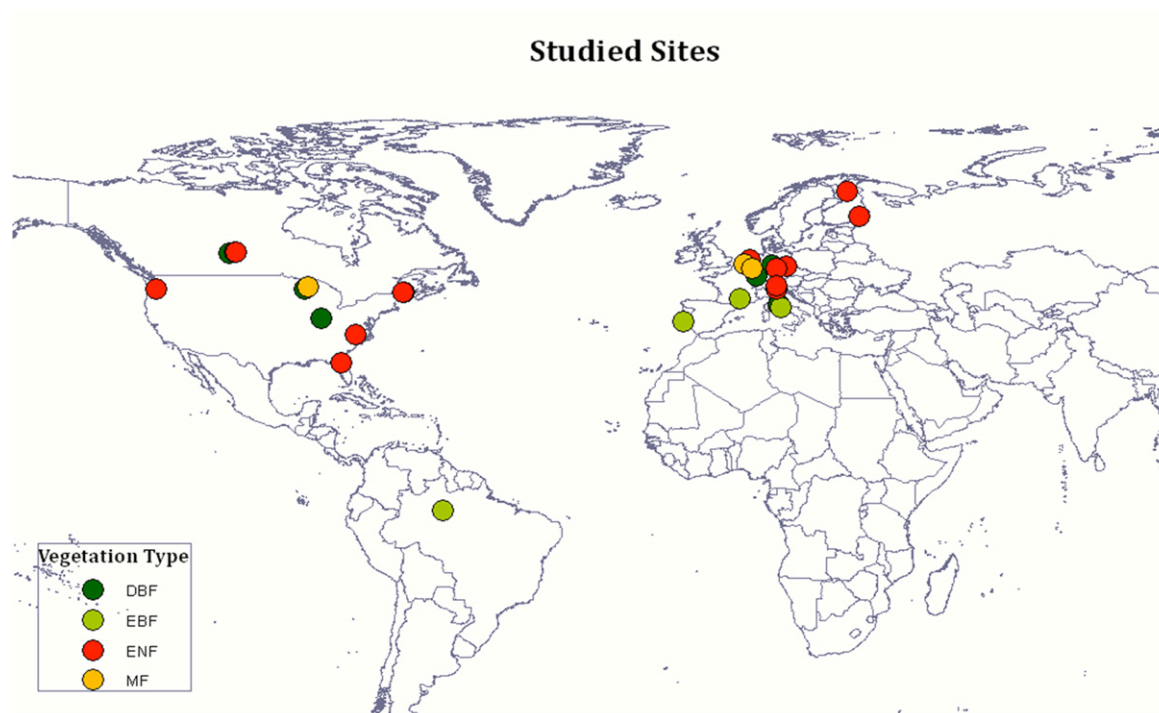


**Figure 1.** Spatial distribution of the studied forest sites. The forest types are shown in the legend. 27 Fluxnet forest sites were used in this analysis, including four evergreen broadleaf forests (EBF), seven deciduous broadleaf forests (DBF), 13 evergreen needleleaf forests (ENF) and three mixed forests (MF). These sites have a minimum of four years of continuous data of gross primary product (GPP), Temperature ( $T_a$ ), Precipitation ( $P$ ), net radiation ( $R_n$ ), Latent heat ( $Le$ ) and Sensible heat ( $H$ ).

vaporization will increase, leading to high EF (Schwalm *et al* 2010). Because of the synthetic nature of EF in characterizing land surface conditions for soil moisture and available energy for plant to use and evaporation, it has been widely used as a drought index (Heim 2002, Nishida (2003)). Here EF is the drought indicator in our analysis.

**2.1.2. MODIS GPP and land cover.** We used global monthly GPP datasets (MOD17A2) provided by Zhao and Running (2010). The MODIS GPP algorithm is used to calculate global GPP with  $0.05 \times 0.05$  degree spatial resolution over the period 2001–2010. Land cover classification (MOD12C1) is defined by the International Geosphere Biosphere Programme (IGBP) global vegetation classification scheme. ([https://lpdaac.usgs.gov/products/modis\\_products\\_table/mcd12c1](https://lpdaac.usgs.gov/products/modis_products_table/mcd12c1)). We masked the areas that are non-forested. ENF, EBF, MF, and DBF were identified based the gridded land cover. ([http://www.mmmt.net/db/0/0/firecenter.umn.edu/pub/NPP\\_Science\\_2010/Monthly\\_MOD17A2/GEOTIFF\\_0.05\\_degree](http://www.mmmt.net/db/0/0/firecenter.umn.edu/pub/NPP_Science_2010/Monthly_MOD17A2/GEOTIFF_0.05_degree)).

## 2.2. CPC

**2.2.1. Forest CPC and PCPC.** The concept of CPC represents the daily maximum carbon assimilation (Yi *et al* 2012). The daily CPC of ecosystems was defined as the maximum value of half-hourly GPP in a day, which was derived from FLUXNET NEE data by nonlinear regression (Reichstein *et al* 2005). A yearly CPC curve is constructed

from daily GPP data (figure 2(a)). This CPC curve forms an upper boundary for the instantaneous canopy photosynthetic rates, and the area under the CPC curve represents ecosystem carbon assimilation potential—how much carbon dioxide potentially can be assimilated by an ecosystem at a site in an individual year. This data-based CPC is in good agreement with modelled photosynthetic capacity ( $A_{max}$ ) (figure 2(a), modelling in details given in the online supplementary materials available at ([stacks.iop.org/ERL/9/065002/mmedia](https://stacks.iop.org/ERL/9/065002/mmedia))). PCPC is defined as a measure of the maximum carbon assimilation potential for a site given site-specific ‘perfect’ climate conditions for a particular day of the year over the years for which data are available. The PCPC values are calculated for each day of the year as the maximum CPC recorded on that day across all available years of site data. Thus, a PCPC curve of maximized carbon assimilation potential can be constructed (figure 2(a)). The difference between PCPC and CPC is defined as CPC deficit (figure 2(a)). We investigate the relationship between magnitudes of the CPC deficit of forests and their driving forces.

**2.2.2. MODIS GPP deficit.** The perfect-deficit approach was also applied to MODIS GPP datasets. The PCPC was calculated as the maximum value of monthly GPP over the years 2001–2010. The CPC deficits were calculated as the difference between monthly PCPC and monthly CPC of specific years.

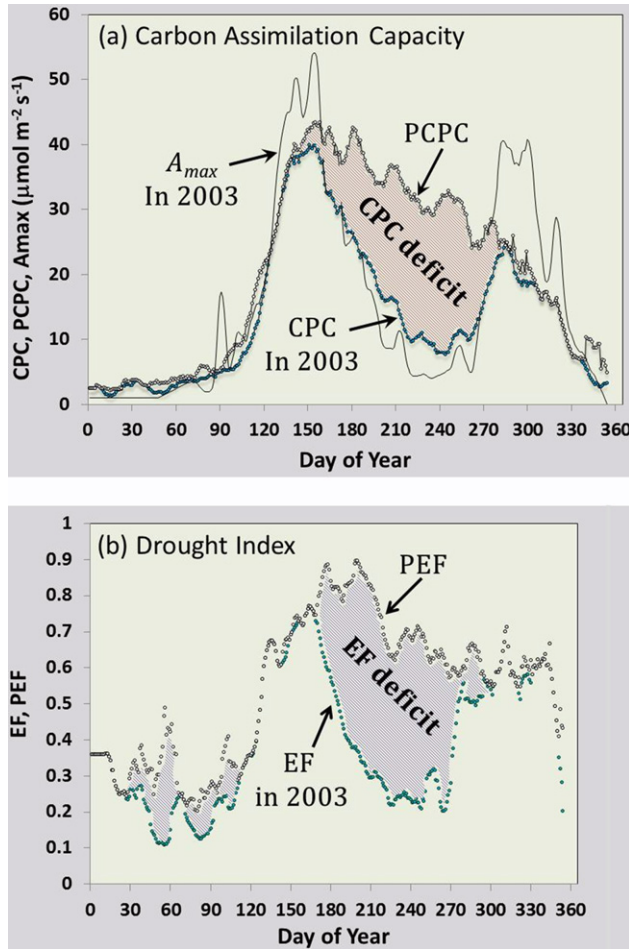


**Figure 2.** Perfect-deficit approach and modeled  $A_{\max}$ . (a) Comparison of CPC, and PCPC by the perfect-deficit approach from flux tower data and modeled photosynthetic capacity  $A_{\max}$ —using the light-response model (Ruimy *et al* 1995, Yi *et al* 2004) (Supplementary Materials). The deficit (shadow) represents the severe GPP drop occurred in growing season 2003 at the IT-Ro2 site located in Italy. PCPC gives the observed site-specific maximum daily GPP rate given ‘perfect’ conditions. (b) Perfect evaporative fraction (PEF) and daily maximum evaporative fraction (EF) in 2003. The shading indicates the EF deficit for that year.

**2.2.3. Climate potential index.** We used a similar approach as above to define climate drivers or drought proxies ( $T_a$ ,  $R_n$ ,  $P$ , VPD, and EF). We extracted the yearly climatic potential curve from the daily maximum observed value of each climate variable for each site-year. Climatic envelopes were defined as the maximum values for each day-of-year observed from at least four continuous yearly records. Climatic drivers are defined as differences between climatic potential and climatic envelopes representing ‘perfect’ climate.

### 2.3. Extreme indices

**2.3.1. Threshold value.** The threshold levels of extremes were defined by the relative monthly CPC deficit  $R_i = (PCPC_i - CPC_i) / PCPC_i$ , here the  $PCPC_i$  is the  $i$ th month PCPC (calculated by integrating daily PCPC), and  $CPC_i$  is  $i$ th month CPC (from integrating the daily CPC).

Based on sensitivity analysis (Supplementary figure 1),  $R_i = 0.3$  is used as a threshold value to identify extreme CPC events. We did piecewise linear regression between  $R_i$  and the fraction of months with relative CPC deficit greater than  $R_i$ . The  $R_i = 0.3$  is close to the break point between a line with steep slope (more sensitive) to one with gentle slope (less sensitive). In order to emphasize severe extreme events and keep results less sensitive to the choice of  $R_i$ , we therefore used  $R_i = 0.3$  as the threshold value. The legitimacy of using  $R_i = 0.3$  as the threshold value in present paper is also evidenced by previously published drought and heat wave events that occurred in 2003 in Europe and caused significant GPP reduction (Ciais *et al* 2005). These documented extreme events can be identified by the choice of  $R_i = 0.3$  as the threshold value in our analysis.

**2.3.2. CPC deficit duration, intensity and severity.** The concept of CPC deficit indices is borrowed from drought terminology (Sheffield and Wood 2007) in which a drought index is calculated as the deficit of soil moisture relative to its seasonal climatology. Similarly, an extreme index from the point of view of the carbon cycle could be calculated as the deficit of CPC relative to its PCPC. An extreme event is defined as a period of duration of  $n$  months with relative deficit ratios larger than an arbitrary level. The departure of CPC from PCPC is the extreme event magnitude  $M_i$  ( $\text{g CO}_2 \text{ m}^{-2}$ ),

$$M_i = PCPC_i - CPC_i, \quad (1)$$

where  $i$  is the  $i$ th month of  $n$  months with  $R_i$  exceeding 0.3 within a May–October period. The mean magnitude over the CPC deficit duration is the intensity  $I$  ( $\text{g CO}_2 \text{ m}^{-2} \text{ month}^{-1}$ ),

$$I = \sum_{i=1}^n M_i / n. \quad (2)$$

The product of duration and intensity gives the CPC deficit severity  $S$  ( $\text{g C m}^{-2}$ ),

$$S = I \times n, \quad (3)$$

or

$$S = \sum_{i=1}^n M_i. \quad (4)$$

We also define classes of extreme events based on their duration as follows:

$D_{1-2}$  ( $1 \leq n \leq 2$ ), short or medium term,  $D_{3-6}$  ( $3 \leq n \leq 6$ ), long term, where the subscript to  $D$  indicates the range of drought duration in months.

### 2.4. Statistical analysis

**2.4.1. PCA.** PCA is a widely used technique in atmospheric sciences. It is a quantitative method to explain the variation of large sets of inter-correlated variables, transforming them into a smaller set of independent (uncorrelated) variables



(principal components). Here, PCA is used to find the correlations between CPC deficits and climate drivers during the northern growing season (May–October). Datasets were standardized before we compute the PCA. We use the first three principal components, which account for at least 70% of the whole dataset variance, to construct plots with axes formed by these three components. The correlations among CPC deficit and climatic drivers were approximately equal to the cosines of the angles between the corresponding lines in the plot (Wilks 2006) (Supplementary figure 2) (This is an approximation because the variance described is 70% and above, rather than 100%).

**2.4.2. Smoothing algorithm.** All of the climatic drivers and model variables were smoothed using a 10 d moving average.

### 3. Results and discussion

As an example, the yearly photosynthetic capacity ( $A_{\max}$ ) curve for site IT-Ro2 (DBF) is constructed from daily data extracted using equation (S1). The physiological meaning of  $A_{\max}$  is the carbon assimilation rate at saturating values of photosynthetic photon flux density. The yearly dynamics of CPC from the perfect-deficit approach and  $A_{\max}$  from the light response model were shown in figure 2(a). Overall, the data-based CPC is consistent with the model-based  $A_{\max}$ . Both CPC and  $A_{\max}$  show the severe carbon assimilation reductions during the 2003 growing season in European DBF sites. However, the modeled  $A_{\max}$  largely overestimates the carbon assimilation around the beginning and end of the growing season, and slightly underestimates it during the growing season. The index EF deficits show the similar pattern as CPC deficit (figure 2(b)). The clear relationship between GPP deficits and EF deficits occurring at the IT-Ro2 site (figures 2(a), (b)) may indicate that drought was the major constraint to growing-season carbon assimilation in this site.

As shown for the example site, we applied the perfect-deficit approach to 27 forest sites covering EBF, DBF, MF and ENF ecosystems to calculate the duration, intensity and severity of CPC deficits. Duration means the number of months with relative deficit above 0.3, intensity was calculated as the mean magnitude of CPC deficit over the duration and severity is the product of intensity and duration (see methods). CPC deficit duration, intensity, and severity for each site are listed in table 1. Severe CPC deficit events, characterized by long duration, were mostly discernible at EBF and DBF sites ( $D_{3-6} > 3$ ). For ENF and MF, only 4.9% and 7.7% of sites exhibit severe CPC deficit events. As shown in figure 3, at the biome scale, the EBF sites were dominated by significant reduction in carbon assimilation indicated by large CPC deficits. Over the studied sites, the EBF CPC deficits were at the highest average severity, with assimilation reduction of  $824.2 \text{ g CO}_2 \text{ m}^{-2}$  per growing season, 1.8 months of duration, and  $415.4 \text{ g CO}_2 \text{ m}^{-2} \text{ month}^{-1}$  of intensity. The average severity, duration and intensity were similar for DBF sites:  $673.2 \text{ g CO}_2 \text{ m}^{-2}$ , 1.5 months, and  $412.3$

$\text{g CO}_2 \text{ m}^{-2} \text{ month}^{-1}$  respectively. The frequency of severe CPC deficit events in the broadleaf forests (i.e. EBF and DBF) indicates high inter-annual variability of carbon assimilation capacity in these ecosystems. In contrast, the ENF sites rarely exhibit significant CPC deficits, with aggregated average values of severity, duration, and intensity of  $149.2 \text{ g CO}_2 \text{ m}^{-2}$ , 0.5 months, and  $186.6 \text{ g CO}_2 \text{ m}^{-2} \text{ month}^{-1}$ , respectively. The three MF sites behaved similarly to the ENF sites. We found that the CPC deficits of forests vary significantly by climate region. The frequency of severe CPC deficits of Mediterranean forests was high (table 1). Because Mediterranean forests usually suffer from long dry summers, drought is the most important cause of forest carbon assimilation declines in this climate zone. There, 75% of the severe CPC deficit events coincide with significant EF deficits.

We applied PCA to illuminate the correlation between CPC deficits and climatic drivers. Conventionally, deconvoluting the climatic effects of carbon assimilation is difficult, because the climatic variables and drought index usually co-vary strongly. PCA methods can effectively separate those effects (Jung *et al* 2007, Wilks 2006). As illustrated in figure 4, CPC deficit of EBF strongly correlates with EF deficit, with a mean correlation coefficient (denoted by cosine of two lines that represent EF deficit and CPC deficit) of 0.42. The cosine values between CPC deficit and other climatic variables ( $T_a$ ,  $R_n$ , VPD and  $P$ ) range from  $-0.04$  to  $0.04$ , indicating very weak correlations. For DBF biomes, the CPC deficit also displayed strong correlation with EF (cosine of 0.43), but slight correlation with  $R_n$  (cosine of 0.18). These results suggest a drought control on CPC in these two broadleaf biomes. However, the correlations of broadleaf forest CPC deficits and precipitation were weak. This may be attributed to several reasons. First, the typical probability density of precipitation is a gamma distribution, while the PCA approach assumes that data is normally distributed. This mismatch may introduce bias to assess the role of precipitation in its correlation to CPC deficits. Second, precipitation is a sporadic input to the soil moisture budget (Noy-Meir 1973), and does not influence ecosystem activities immediately. In addition, compared to herbaceous vegetation, trees are generally more resistant to instantaneous local environmental changes (Teuling *et al* 2010) because they can access deep soil moisture and groundwater, which smooth out variability in response to precipitation.

A number of previous studies have suggested that, in temperate boreal forest ecosystems, the growing season photosynthetic capacity is mostly constrained by temperature (Falge *et al* 2002, Griffis, Black 2003). Indeed, the correlation of the CPC deficits in both ENF and MF with climatic drivers was weak (figure 4). The correlation between ENF CPC deficit and  $R_n$  was highest (cosine 0.26) out of the climatic drivers, while the MF CPC deficit had no significant correlation with any of the climate drivers or with EF.

Within the same type of forest, the climatic control of carbon assimilation capacity could vary among climatic zones (Supplementary table 1). The CPC deficits of Mediterranean EBF (Csa) was apparently controlled by drought while that of

**Table 1.** Forest flux towers used in this study and the number of long term CPC deficit events (over May–October) in each.

Site code	Site name	Lat	Lon	Veg	Climate	Years	Severe CPC deficit events	Duration (months)	Severity (g CO <sub>2</sub> m <sup>-2</sup> )	Intensity (g CO <sub>2</sub> m <sup>-2</sup> month <sup>-1</sup> )
US-MMS	Morgan Monroe State Forest	39.32	86.41	DBF	Cfa	2000–2005	—	0.5	115.1	230.2
DE-Hai	Hainich	51.08	10.45	DBF	Cfb	2001–2006	—	0.7	224.3	336.5
FR-Hes	Hesse Forest-Sarrebourg	48.67	7.06	DBF	Cfb	2001–2006	3(2003–2005)	2.0	1171.3	585.7
IT-Ro1	Roccarespanni1	42.49	11.93	DBF	Csa	2001–2006	3(2001,2003,2004)	2.2	946.1	436.7
IT-Ro2	Roccarespanni2	42.39	11.92	DBF	Csa	2002–2006	2(2003,2004)	1.6	956.3	597.7
US-Wcr	Willow Creek	45.81	−90.08	DBF	Dfb	2001–2006	1(2001)	1.7	719.3	431.6
CA-Oas	SK-Old Aspen	53.63	−106.2	DBF	Dfc	2000–2005	1(2003)	2.2	579.9	267.6
	Average							1.5	673.2	412.3
BR-Ma2	Manaus—ZF2 K34	−2.61	−60.3	EBF	Af	2002,2002,2004–2006	1(2002)	2.0	1276.3	638.2
FR-Pue	Puechabon	43.74	3.59	EBF	Csa	2001–2006	2(2005,2006)	2.5	1171.3	468.5
IT-Cpz	Castelporziano	41.71	12.37	EBF	Csa	2001–2006	2(2001,2006)	2.3	795.7	341.0
PT-Esp	Espirra	38.64	−8.6	EBF	Csa	2002–2004, 2006	—	0.3	53.5	214.1
	Average							1.8	824.2	415.4
US-Dk3	Duke Forest Loblolly Pine	35.97	−79.09	ENF	Cfa	2002–2005	—	0.0	0.0	0.0
US-Sp3	Donaldson	29.75	−82.16	ENF	Cfa	2001–2004	—	0.5	223.2	446.4
DE-Tha	Harandt	50.96	13.57	ENF	Cfb	2001–2006	—	0.3	119.1	357.4
DE-Wet	Wetzstein	50.45	11.45	ENF	Cfb	2002–2006	—	0.6	214.1	356.9
IT-Lav	Lavarone	45.95	11.28	ENF	Cfb	2001–2002,2004,2006	—	0.0	0.0	0.0
NL-Loo	Loobos	52.17	5.74	ENF	Cfb	2001–2006	—	0.0	0.0	0.0
IT-Sro	San Rossore	46.58	11.43	ENF	Csa	2001–2006	1(2003)	1.3	448.1	336.1
US-Wrc	Wind River Crane Site	45.82	−121.95	ENF	Csb	2000–2002,2004,2006	2(2000, 2006)	1.6	657.3	410.8
US-Ho1	Howland Forest	45.2	−68.74	ENF	Dfb	1999–2004	—	0.0	0.0	0.0
US-Ho2	Howland Forest	45.21	−68.75	ENF	Dfb	1999–2004	—	0.0	0.0	1.0
CA-obs	SK-Southern Old Black Spruce	53.99	−105.12	ENF	Dfc	2000–2005	—	0.5	87.1	174.2
CA-ojp	SK-Old Jack Pine	53.9	−104.69	ENF	Dfc	2000–2005	—	0.8	127.9	153.5
FI-Hyy	Hyttiala	61.84	29.29	ENF	Dfc	2001–2006	—	0.3	63.1	189.4
	Average							0.5	149.2	186.6
BE-Bra	Brasschaat	51.31	4.52	MF	Cfb	2000,2002,2004–2006	1(2002)	2.0	629.8	314.4
BE-Vie	Vielsalm	50.3	5.99	MF	Cfb	2001–2004,2006	—	0.0	0.0	0.0
US-Syv	Sylvania Wilderness Area	46.242	−89.35	MF	Dfb	2002–2005	—	1.0	154.1	154.1
	Average							1.0	261.3	156.2

Severe CPC deficit events are defined as three consecutive months with relative deficit ratio (monthly CPC deficit divided by PCPC) exceeding 0.3 ( $D > 3$ ). Severe CPC deficit events were mostly discernible at EBF and DBF sites. Climate grouping follows the Köppen–Geiger classification scheme: A, moist tropical climate, with Af indicating tropical rain forest; C, moist climate with mild winters: Cfa and Cfb represent humid subtropical climate, Csa and Csb represent Mediterranean climate; D, moist climates with severe winters: Dfb represents humid continental climate and Dfc represents subpolar climate.

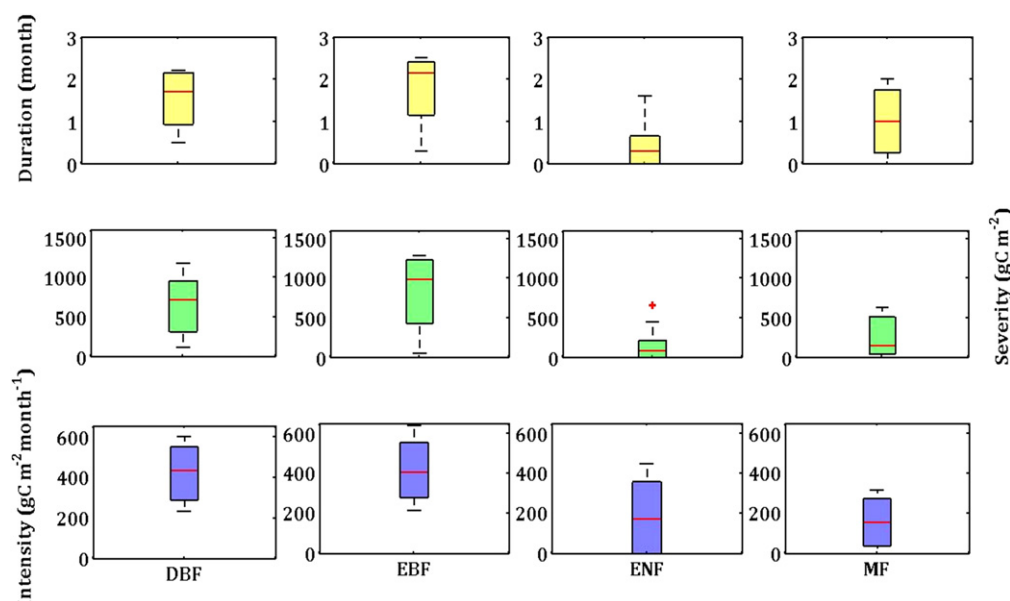


**Figure 3.** Duration, intensity and severity of CPC deficit of Fluxnet forest sites (per growing season). Shown are the median (red horizontal lines), the quartiles (colored boxes), 25th and 75th percentiles (the edges of the box). Duration counts the months with relative deficit ratio exceeding 0.3 for each growing season. Magnitude indicates the sum of the differences between monthly PCPC and CPC. Mean magnitude (the value of magnitude over duration) is defined as intensity. The product of duration and intensity gives the CPC deficit severity.

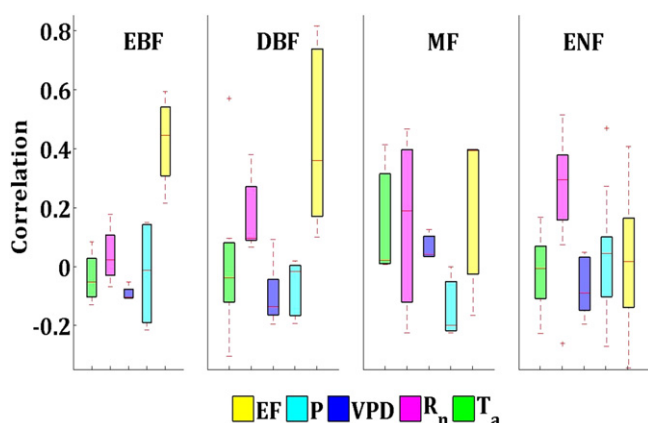


**Figure 4.** Correlations between CPC deficits and climatic variable deficits (May–October). Shown are the median (red horizontal lines), the quartiles (colored boxes), 25th and 75th percentiles (the edges of the box). The correlations are calculated using principal component analysis. Three components are retained to form three dimensional plots, which explain at least 70% of total variations of the dataset (Supplementary table 2). Correlations are calculated as the cosines of the angles between GPP deficits and Temperature ( $T_a$ ), Radiation ( $R_n$ ), vapor pressure deficit (VPD), Precipitation ( $P$ ), Evaporative Fraction (EF) deficits. CPC deficits of DBF and EBF are highly correlated with EF deficits, suggesting drought control of carbon sequestration among these two types of forests.

tropical (Af) EBF depended less on climatic factors. In contrast to Mediterranean (Csa) DBF, whose carbon assimilation capacity exhibited a strong dependence on drought, continental and moist tropical DBF (Cfb and Dfb) carbon assimilation capacities were less impacted by drought. Instead,  $T_a$  and radiation were stronger constraints.

Figure 5 illustrates the monthly global spatial extent of CPC deficits during the growing season. Non-forested areas

are masked from the analysis. We estimate a climate-attributable global reduction of forest CPC of 6.3 Pg C ( $\sim 5.2\%$  of total terrestrial GPP) per growing season, and EBF forests contributed 51.7% of the total reduction. Although DBF displayed significant CPC deficits at the site level, the total carbon lost was small due to the small area this biome covered globally. The high CPC deficits of EBF occur in August and September, especially at the tropical forests of Brazil. The large CPC deficits in temperate and boreal forests (ENF and MF) occurred in May, most pronounced at boreal forests of Canada, northern United States, and western Russia. The ENF and MF biomes together contribute almost half of total forest carbon assimilation reduction.

## 4. Conclusions

We analyzed the effects of climate extremes on forest carbon assimilation and discussed how that might impact the carbon cycle. An observation-based estimate of those impacts was presented by introducing three indices of assimilation deficit periods: duration, intensity and severity. Our study suggests that carbon assimilation capacities of broadleaf forests (EBF and DBF) could be significantly impacted by drought, indicated by low values of EF. On the global scale, EBF contributes more than 50% of the carbon reduction of forests. Climate extreme events, specifically drought, are expected to increase in intensity and severity in the future. The present analysis can help identify and quantify the impacts of climate extremes on terrestrial carbon cycles and improve our understanding of carbon-climate feedback mechanisms.



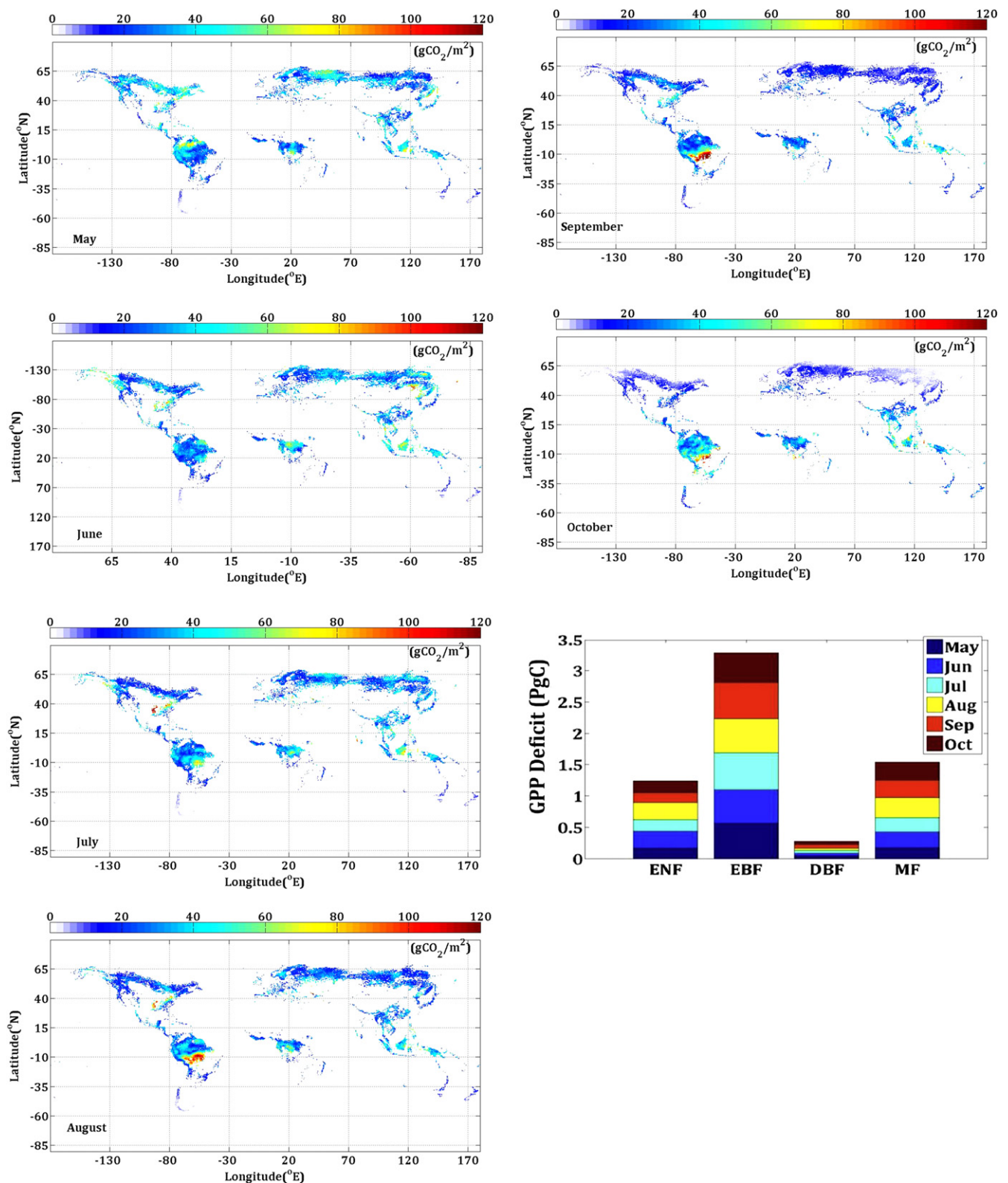


**Figure 5.** Remotely sensed GPP deficit over May–October. GPP deficits through 2001–2013 are aggregated into monthly means. In this study, we used global MODIS GPP datasets published in Zhao and Running (2010) to calculate GPP deficits by perfect-deficit approach (Yi *et al* 2012). Forest GPP was calculated based on MOD12C1 land cover product. Non-forested areas were masked from our analysis.

## Acknowledgements

CY was supported by the US National Science Foundation under grant NSF-DEB-0949637. We thank Dr Maosheng Zhao for providing the MODIS17A2 GPP data for this research. We also thank FLUXNET site PIs for contributing data, and the agencies and institutions that funded long-term measurements at these sites. NYK was supported by NOAA under grants NA11SEC4810004 and NA12OAR4310084. All statements made are the views of the authors and not the opinions of the funders or government.

## References

- Allen C D *et al* 2010 A global overview of drought and heat-induced tree mortality reveals emerging climate change risks for forests *Forest Ecol. Manag.* **259** 660–84
- Bonan G B 2008 Forests and climate change: forcings, feedbacks, and the climate benefits of forests *Science* **320** 1444
- Ciais P *et al* 2005 Europe-wide reduction in primary productivity caused by the heat and drought in 2003 *Nature* **437** 529–33
- Cox P M, Betts R A, Jones C D, Spall S A and Totterdell I J 2000 Acceleration of global warming due to carbon-cycle feedbacks in a coupled climate model *Nature* **408** 184–7
- Dai A 2011 Drought under global warming: a review *Wiley Interdiscip. Rev.: Clim. Change* **2** 45–65
- Falge E *et al* 2002 Seasonality of ecosystem respiration and gross primary production as derived from FLUXNET measurements *Agric. Forest Meteorol.* **113** 53–74
- Friedlingstein P *et al* 2006 Climate-carbon feedback analysis: results from the C4MIP model intercomparison *J. Clim.* **19** 3337–53
- Gielen B *et al* 2013 Biometric and eddy covariance-based assessment of decadal carbon sequestration of a temperate Scots pine forest *Agric. Forest Meteorol.* **174** 135–43
- Griffis T J and Black T A 2003 Eco-physical controls on the carbon balances of three southern boreal forests *Agric. Forest Meteorol.* **117** 53–71
- Jung M *et al* 2007 Uncertainties of modeling gross primary productivity over Europe: a systematic study on the effects of using different drivers and terrestrial biosphere models *Glob. Biogeochem. Cycles* **21** GB 4021
- Meehl G A and Tebaldi C 2004 More intense, more frequent, and longer heat waves in the 21st century *Science* **305** 994
- Mu Q, Zhao M and Running S W 2011 Improvements to a MODIS global terrestrial evapotranspiration algorithm *Remote Sens. Environ.* **115** 1781–800
- Nemani R *et al* 2003 Climate-Driven increases in global terrestrial net primary production from 1982 to 1999 *Science* **300** 1560
- Nishida K 2003 An operational remote sensing algorithm of land surface evaporation *J. Geophys. Res.* **108** 4270
- Noy-Meir I 1973 Desert ecosystem. I. environment and producers *Annu. Rev. Ecol. Syst.* **4** 25–52
- Papale D *et al* 2006 Towards a standardized processing of net ecosystem measured with eddy covariance technique: algorithms and uncertainty estimation *Biogeosci.* **3** 571–83
- Reichstein M *et al* 2005 On the separation of net ecosystem exchange into assimilation and ecosystem respiration: review and improved algorithm *Glob. Change Biol.* **11** 1424–39
- Ruimy A, Jarvis P G, Baldocchi D D and Saugier B 1995 CO<sub>2</sub> fluxes over plant canopies and solar radiation: a review *Adv. Ecol. Res.* **26** 1–68
- Schwalm C R *et al* 2010 Assimilation exceeds respiration sensitivity to drought: a FLUXET synthesis *Glob. Change Biol.* **16** 657–70
- Sheffield J and Wood E 2007 Global trends and variability in soil moisture and drought characteristics 1950–2000, from observation-driven simulations of the terrestrial hydrological cycle *J. Clim.* **21** 432–58
- Teuling A *et al* 2010 Contrasting response of European forest and grassland energy exchange to heatwaves *Nat. Geosci.* **3** 722–7
- Trenberth K E 2012 Framing the way to relate climate extremes to climate change *Clim. Change* **115** 283–90
- Vicente-Serrano S M *et al* 2013 Response of vegetation to drought timescales across global land biomes *Proc. Natl. Acad. Sci. USA* **110** 52–7
- Wilks D S 2006 *Statistical Methods in the Atmospheric Sciences* (New York: Academic Press) p 506
- Yi C *et al* 2004 A nonparametric method for separating photosynthesis and respiration components in CO<sub>2</sub> flux measurements *Geophys. Res. Lett.* **31** L17107
- Yi C *et al* 2010 Climate control of terrestrial carbon exchange across biomes and continents *Environ. Res. Lett.* **5** 034007
- Yi C *et al* 2012 Climate extremes and grassland potential productivity *Environ. Res. Lett.* **7** 035703
- Yi C, Ricciuto D and Hendrey G 2013 Biome Q10 and dryness *Am. J. Clim. Change* **2** 292–5
- Zhao M and Running S W 2010 Drought-induced reduction in global terrestrial net primary production from 2000 through 2009 *Science* **329** 940–3